Impedance Eduction in Large Ducts Containing Higher-Order Modes and Grazing Flow

Willie R. Watson* and Michael G. Jones†

NASA Langley Research Center, Hampton, Virginia 23681-2199

Impedance eduction test data are acquired in ducts with small and large cross-sectional areas at the NASA Langley Research Center. An improved data acquisition system in the large duct has resulted in increased control of the acoustic energy in source modes and more accurate resolution of higher-order duct modes compared to previous tests. Two impedance eduction methods that take advantage of the improved data acquisition to educe the liner impedance in grazing flow are presented. One method measures the axial propagation constant of a dominant mode in the liner test section (by implementing the Kumarsean and Tufts algorithm) and educes the impedance from an exact analytical expression. The second method solves numerically the convected Helmholtz equation and minimizes an objective function to obtain the liner impedance. The two methods are tested first on data synthesized from an exact mode solution and then on measured data. Results show that when the methods are applied to data acquired in the larger duct with a dominant higher-order mode, the same impedance spectra are educed as that obtained in the small duct where only the plane wave mode propagates. This result holds for each higher-order mode in the large duct provided that the higher-order mode is sufficiently attenuated by the liner.

I. Introduction

INCREASINGLY stringent international noise constraints have resulted in continued emphasis on development of improved technologies to reduce the overall level of fan noise radiated to communities that surround airports. Although locally-reacting sound absorbing structures (acoustic liners) mounted in the aircraft engine nacelles currently provide significant fan-noise reduction, further optimization is required to increase their noise reduction capacity and bandwidth. The critical intrinsic parameter used in this optimization is the locally-reacting acoustic impedance of the liner. Therefore, an accurate knowledge of this quantity is critical for the design of quieter aircraft.

*Senior Research Scientist, Research Directorate, Computational AeroSciences Branch, Liner Physics Group, Associate Fellow AIAA.

†Senior Research Scientist, Research Directorate, Structural Acoustics Branch, Liner Physics Group, Associate Fellow AIAA.

The acoustic impedance is defined as the ratio of the acoustic pressure to the normal component of acoustic particle velocity at the surface of the liner. Because of the difficulty with measuring these two quantities (i.e., acoustic pressure and acoustic particle velocity) at the liner surface, a measurement of acoustic impedance is problematic at best. Instead, a number of indirect methods (i.e., a combination of measurement and numerical computation) have been developed for this purpose.

For nearly 30 years, the NASA Langley Research Center has invested a significant effort in the development of indirect impedance prediction tools and experimental rigs for the evaluation of acoustic liner impedance.[1–6] This has included the development of prediction tools to account for the effects of both uniform and shear flow profiles in the duct. These tools are applicable to rectangular ducts for which the test liner is mounted in one wall while the remaining walls remain rigid. These tools have the additional restriction that the cross-sectional area of the flow duct must be sufficiently small, so that at the targeted frequencies the sound field between the two rigid walls adjacent to the liner consists of only the plane wave mode. When applied to Langley facilities, these impedance eduction tools are only applicable to test liners installed into the NASA Langley Grazing Flow Impedance Tube (GFIT).[2] The NASA Langley Curved Duct Test Rig (CDTR)[7,8] has a much larger flow path that is comparable in size to the nacelles found in a small business jet. Because this larger measurement apparatus allows for higher-order duct modes to propagate in hard wall sections without decay (i.e., to be cut on), the aforementioned impedance eduction tools[1–6] are not directly transferable to the CDTR.

In a recent paper,[9] a single mode theory for impedance eduction in a large duct such as the CDTR was presented. The fundamental assumption of the theory is that a single, higher-order mode is dominant between the two rigid walls adjacent to the test liner and that the test sample has a uniform impedance. The Kumaresan and Tufts (KT) algorithm[10,11] is used to determine an axial propagation constant in the liner test section and a closed-form solution is used to educe the liner impedance from this measured axial propagation constant. Three shortcomings of the single mode theory for impedance eduction in the CDTR were highlighted in the previous paper.[9] First, the control system in the CDTR was only able to drive a dominant higher-order mode down the duct for slightly more than half of the test frequencies of interest. Secondly, although the educed impedance spectra for each high-order mode driven down the CDTR should be identical to that of the plane wave mode, this could only be demonstrated for a few higher-order modes. Finally, the single mode theory does not allow test samples with nonuniform surface impedance, while nonuniform surface impedance liners have a broader sound attenuation bandwidth and are more desirable for fan noise reduction.

In the last few years, the number of loudspeakers (i.e., drivers) in the control system has been doubled to provide increased control authority over the source modes in the CDTR. This should improve the ability to perform impedance eduction over the full range of test frequencies. Second, improvements in the resolution of higher-order duct modes are obtained by adding thirty-two addi-

tional microphones to the CDTR measurement system. This should allow better comparison of the educed impedance between the plane wave and higher-order mode sources. Third, an additional impedance eduction method that is less restrictive than the single mode method (because it allows for variable impedance liners) has been developed for use in the CTDR. This less restrictive method is presented in this paper. The two impedance eduction methods are tested in a duct with a small cross-sectional area (i.e., the GFIT) and in a duct with a large cross-sectional area (i.e., the CDTR). For the test conditions of interest, only the plane wave horizontal and vertical modes are cut on in the hard wall sections of the GFIT while several higher-order horizontal and vertical modes are cut on in the hard wall sections of the CDTR. (Note: The test liner is inserted into the top wall in the GFIT and into the sidewall in the CDTR. Hence, the horizontal mode in the GFIT and the vertical mode in the CDTR are both between the rigid walls adjacent to the liner in their respective test rigs). Exact data (from mode analysis) and measured data (from experimental tests) are used to test the efficacy of these impedance eduction techniques in both the small and large duct. This is achieved by demonstrating that the methods educe the same locally-reacting impedance for a test sample that is placed in the small and large duct regardless of whether higher-order modes are cut on in the large duct.

II. Description of Test Facility and Test Set-up

The GFIT and its instrumentation are fully described in several earlier papers,[2,5,6] so only the CDTR and its instrumentation is described in detail in this paper. Figure 1 is a photograph of the CDTR. The figure shows the loudspeaker source section, the upstream microphone section, the

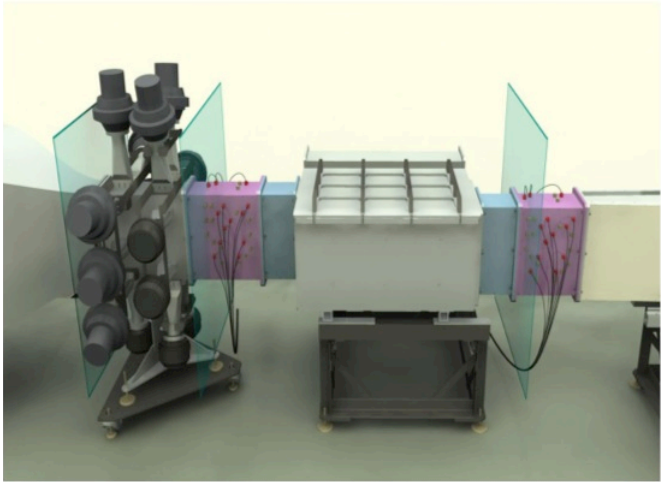

Figure 1. Curved Duct Test Rig test section showing the sound source, the upstream and downstream microphone arrays, and the liner test section.

liner test section, and the downstream microphone section. Mean flow is from left to right and sound in the duct is generated by the array of loudspeakers. The magnitude and phase of the voltage signal to each loudspeaker is controlled such that a selected mode can be generated in the duct. The recorded signals from upstream and downstream microphone arrays are analyzed to determine the mode distribution of the sound in the duct incident upon and discharged from the liner test section. The control system is designed not only to generate a selected mode but also to suppress all other modes in the duct. Thus, the sound incident on the liner is expected to be predominantly composed of the selected mode, which is expected to be at least 10 dB greater than any other mode in the duct. Although Fig. 1 shows an array of only sixteen loudspeakers as in previous tests, the number of loudspeakers for the current tests have been increased to thirty-two to provide more control authority over the source modes. To provide better resolution of high-order duct modes, the number of microphones in both the upstream and downstream arrays has been increased from forty-seven to sixty-three for the current tests.

The sound wave incident on the liner test section consists of a tone generated in the duct at 130 dB. Sound waves in the hard wall section are controlled to have at most three horizontal modes ($n = 0, 1, 2$) and seven vertical modes ($m = 0, 1, 2, 3, 4, 5, 6$). Throughout this paper the modes are designated as (n, m), where n is the horizontal and m is the vertical mode order. For this test, either the (0,0), (0,1), or (0,2) mode is generated in the hard wall section upstream of the liner test section as the sound source. The liner test section is a duct of 0.81 m $\times$ 0.38 m cross-section and the liner sample, which is assumed to be uniform and locally-reacting comprises a portion of the right sidewall of the duct. The wall opposite the liner is fully rigid, as are the top and bottom walls of the duct. In the top wall of the duct is a linear array of microphones that span the length of the test liner. Figure 2 shows the liner test section with the straight liner installed on the right sidewall and the hard wall opposite. The lid, which contains the linear microphone array, has been

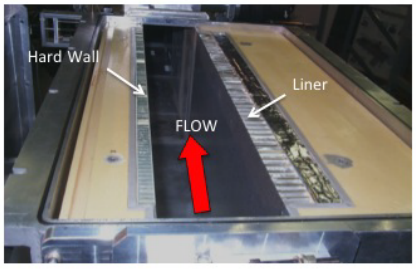

Figure 2. The Curved Duct Test Rig liner test section showing the liner sample on right sidewall, the hard wall opposite the test liner, and the top wall removed.

removed for this photograph, but is shown in the photograph of Fig. 3.

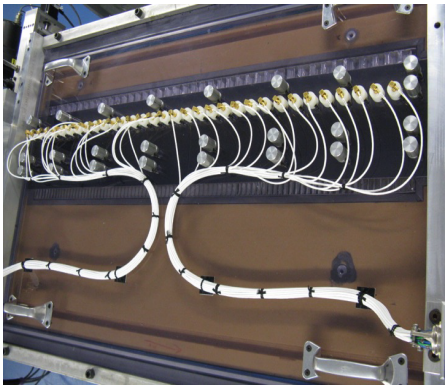

Figure 3. Photograph of Curved Duct Test Rig lid microphone array.

III. Description of Flow Duct and Coordinate System

A schematic of the portion of the CDTR flow duct that is used in this analysis is shown in Fig. 4. The mean flow field is assumed constant with Mach number, M, and is directed from left to

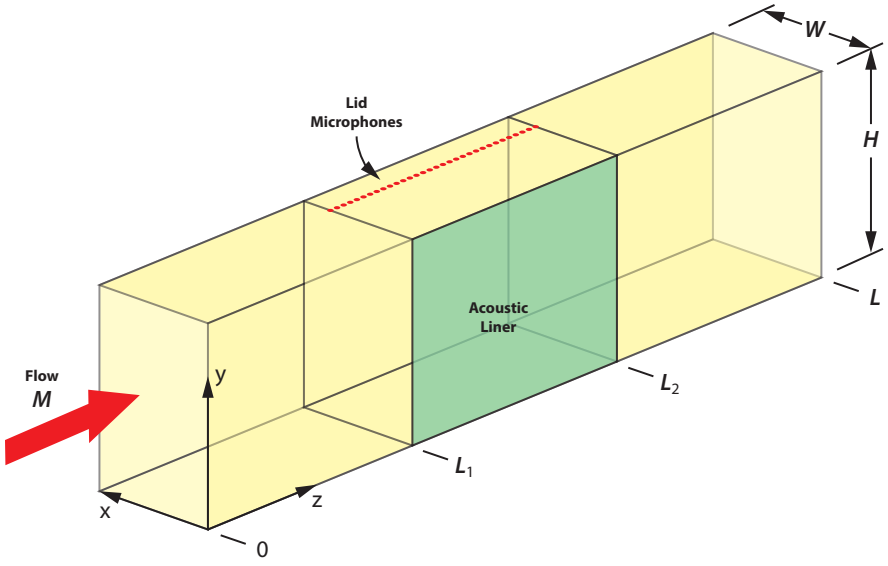

Figure 4. Schematic of 3D flow duct and Cartesian coordinate system.

right along the axis of the duct. The origin of the coordinate system is in the lower right corner of the flow duct, 0.58 m upstream of the leading edge of the liner (L_1 =0.58 m) as shown. Further, the exit plane is located 0.20 m downstream of the trailing edge of the liner ($L - L_2$=0.20 m). The liner sample is 0.81 m in length ($L_2 - L_1$=0.81 m) and its unknown normalized impedance is assumed constant and denoted by ζ. As shown in Fig. 4, there is a single linear array of microphones mounted in the lid of the CDTR. This array consists of thirty-two equally spaced microphones that

are 2.54 cm apart. The linear array is located $2W/3$ units from the right sidewall with the first and last microphone located at the leading and trailing edges of the liner, respectively. The single mode method educes the unknown normalized impedance, ζ, of the test sample using acoustic pressure data obtained only from the lid microphones. As stated earlier, there are sixty-three microphones in both the upstream and the downstream hard wall sections, but they are not shown in Fig. 4. The goal of the other impedance eduction method is to educe the impedance with all 158 microphones (63 microphones in the upstream microphone array, 63 microphones in the downstream microphone array, and 32 microphones in the lid). The following section gives a brief description of each of the impedance eduction techniques that have been implemented in the CDTR.

IV. Impedance Eduction Techniques

Two impedance eduction techniques are described in this section: the Single Mode (SM) method and the Convected Helmholtz Equation (CHE) method. The SM method is a direct method (i.e., the impedance is educed using the measured data without an iterative process). The CHE method is an indirect method (i.e., the impedance is educed via an iterative process using the measured data). Each of these methods have been implemented into the CDTR. Because both of these methods are described in other papers, only enough detail is included in this section to provide both continuity and clarity with the result section of this paper.

A. The SM Method

When the liner impedance is uniform and the sound energy in the liner test section resides in a dominant vertical mode (between the two rigid walls adjacent to the liner), the acoustic pressure field, $p(x,y,z)$, in the liner test section can be expanded as a series of hard wall duct modes in the vertical (i.e., y) coordinate [9]

$$p(x,y,z) = \sum_{n=0}^{nmax} A_{nm}^{\pm} p_{nm}^{\pm}(x) \cos(\frac{m\pi y}{H}) e^{-iK_{nm}^{\pm} z}, \quad p_{nm}^{\pm}(x) = \cos(\lambda_{nm}^{\pm} x) \tag{1}$$

The eigenvalues, $\lambda_{nm}^{\pm}$, and axial propagation constants, $K_{nm}^{\pm}$, are related by the dispersion relation

$$\left(\lambda_{nm}^{\pm}\right)^2 = k^2 - (1-M)^2 \left(K_{nm}^{\pm}\right)^2 - \left(\frac{m\pi}{H}\right)^2 - 2kMK_{nm}^{\pm} \tag{2}$$

The above expressions (i.e., Eqs. (1) and (2)) holds in both hard wall duct segments for which $\frac{1}{\zeta} = 0$, and soft wall duct segments for which $\frac{1}{\zeta} \neq 0$. For a specified wall impedance, ζ, the axial propagation constants, $K_{nm}^{\pm}$, and duct eigenvalues, $\lambda_{nm}^{\pm}$, are obtained from the solution to the exact

transcendental equation

$$ikW\left(1-\frac{MK_{nm}^{\pm}}{k}\right)^2-\zeta(\lambda_{nm}^{\pm}W)\tan\left(\lambda_{nm}^{\pm}W\right)=0 \tag{3}$$

Conversely, if an axial propagation constant is known for a single mode, then the impedance can be determined from a closed-form solution to Eq. (3)

$$\zeta=\frac{ik\left(1-\frac{MK_{nm}}{k}\right)^2}{\sqrt{(k-K_{nm}M)^2-(K_{nm})^2-\left(\frac{m\pi}{H}\right)^2}\tan\left(W\sqrt{(k-K_{nm}M)^2-(K_{nm})^2-\left(\frac{m\pi}{H}\right)^2}\right)} \tag{4}$$

For the preceding equations, m is the dominant vertical mode order, n is the horizontal mode order, *nmax* is chosen large enough so that all cut on modes are included in the mode series, and the superscript $\pm$ denotes right and left-running modes, respectively. The $A_{nm}^{\pm}$'s are the complex mode coefficients and $p_{nm}^{\pm}(x)$ is the normal acoustic pressure mode between the rigid and lined wall. Further, $k=2\pi f/c$ is the free space wavenumber, f is the source frequency in Hertz, c is the speed of sound in the duct, and the superscript $\pm$ has been dropped from the right-hand side of Eq. (4) for the sake of brevity. In the SM method, the lid microphones are used to measure an axial propagation constant, K_{nm}, and Eq. (4) is used to determine the impedance. In a previous paper,[6] a Prony method was used to measure K_{nm}. A more robust KT algorithm[11] has been implemented in this paper to measure K_{nm}. Therefore, the SM method as used in this paper is referred to as the KT algorithm method.

B. The CHE Method

The CHE method for impedance eduction was presented in a previous paper.[9] Because the upper and lower walls of the CDTR are rigid, the acoustic pressure field in the vertical (i.e., the y) coordinate is expanded as a series of hard wall duct modes:

$$p(x,y,z)=\sum_{m=0}^{m=\infty}P_m(x,z)\cos\left(\frac{m\pi y}{H}\right) \tag{5}$$

The equation that describes the propagation of each vertical mode is the quasi-3D convected Helmholtz equation (CHE):

$$(1-M^2)\frac{\partial^2P_m(x,z)}{\partial z^2}+\frac{\partial^2P_m(x,z)}{\partial x^2}-2ikM\frac{\partial P_m(x,z)}{\partial z}+\left[k^2-\left(\frac{m\pi}{H}\right)^2\right]P_m(x,z)=0 \tag{6}$$

The sound source, $p_s(x)$, is measured so that the source boundary condition for the dominant vertical mode, m, is:

$$P_m(x,0) = p_s(x) \tag{7}$$

Similarly, at the exit plane ($z = L$) the exit pressure, $p_e(x)$, is also measured:

$$P_m(x,L) = p_e(x) \tag{8}$$

The left sidewall is rigid so that the boundary condition is:

$$\frac{\partial P_m(W,z)}{\partial x} = 0 \tag{9}$$

Finally, the test liner is assumed locally reacting so that the appropriate wall impedance boundary condition[12] is

$$\frac{\partial P_m(0,z)}{\partial x} = ik\frac{P_m(0,z)}{\zeta} + 2M\frac{\partial}{\partial z}\left[\frac{P_m(0,z)}{\zeta}\right] + \frac{M^2}{ik}\frac{\partial^2}{\partial z^2}\left[\frac{P_m(0,z)}{\zeta}\right] \tag{10}$$

In Eq. (10), the liner impedance may vary with the axial location but is otherwise constant. At this point, the CHE method parallels that presented in an earlier paper[1] for the plane wave mode. However, the vertical mode order chosen is not the $m = 0$ vertical mode order as in the GFIT but the dominant vertical mode in the CDTR. Equations (6)−(10) are solved numerically by using a cubic finite-element method with the dominant vertical mode as the vertical mode order, m. An objective function, $\Phi(\zeta)$, is then formed from the microphone measurements in the CDTR:

$$\Phi(\zeta) = \frac{1}{N}\sum_{I=1}^{N} || \, p(x_I,y_I,z_I) - P_m(x_I,z_I)\cos\left(\frac{m\pi y_I}{H}\right) || \tag{11}$$

where $||\ \ ||$ denotes the magnitude of a complex quantity, $N = 158$ is the number of microphones in the CDTR, and the spatial locations (x_I,y_I,z_I) are the microphone locations in the duct. Further, $p(x_I,y_I,z_I)$ and $P_m(x_I,z_I)\cos\left(\frac{m\pi y_I}{H}\right)$ are the measured and the finite element computed acoustic pressure fields, respectively, at the microphone locations. The objective function, $\Phi(\zeta)$, is minimized using a Davidon-Fletcher Powell optimization algorithm[13] and the impedance that minimizes $\Phi(\zeta)$ is the impedance of the test liner.

V. The Test Liner

Two single-layer, perforate-over-honeycomb liner samples are used in this study. Both samples are tested at two nominal centerline Mach numbers (Mach 0.0, and Mach 0.3). One sample was fabricated to fit the test section of the GFIT and the other sample was fabricated to fit the test

section of the CDTR. These liner samples are representative of single-degree-of-freedom liners currently used in aircraft engine noise reduction. Figure 5 is a schematic of a typical liner sample.

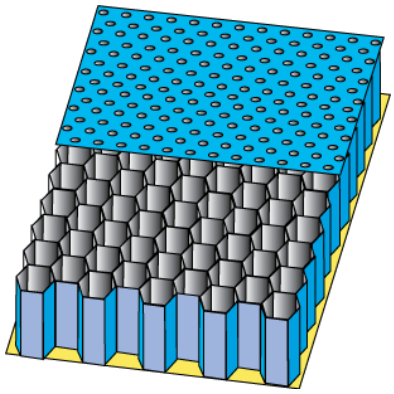

Figure 5. Schematic of the single-layer, perforate-over-honeycomb liner.

The GFIT liner sample is 51 mm wide and 406 mm long, whereas the CDTR sample is 381 mm wide and 813 mm long. Each liner sample consists of a 38.1 mm deep honeycomb core (i.e., $d = 38.1$ mm) bonded on the backside to a 1 mm thick solid sheet and on the flow side to a 1 mm thick perforated plate. The perforate is 8.7% open area and the holes in the plate are 1 mm diameter. The expectation is that the impedance spectra educed in each flow duct is the same for the KT algorithm method and for the CHE method. The impedance educed in the two flow ducts (GFIT and CDTR) should be nearly identical if the higher-order mode impedance eduction methodologies are valid.

VI. Results and Discussion

In this section, the KT algorithm and the CHE impedance eduction methods are tested under the assumption of uniform mean flow. Results are computed for the duct with small cross-sectional area (i.e., the GFIT) and for the duct with a much larger cross-sectional area (i.e., the CDTR). First, the impedance eduction methods are tested utilizing data synthesized from the exact mode solution for right-moving modes given in Eq. (1). Of the many right-moving duct modes that are available, we will target only the least-attenuated mode in the mode series of Eq. (1). The least attenuated mode is defined as the one that suffers the least amount of attenuation as it propagates from left to right along the duct. It is generally the most important mode because it is expected to carry a significant amount of the acoustic energy generated by the sound source. The least attenuated, right-moving mode coefficient, A^+_{nm}, is set to a 130 dB sound pressure level (A^+_{nm}=63.25 Pa). This exact solution affords one the opportunity to test the impedance eduction methodologies in both ducts when they are free from measurement uncertainties and boundary layer effects. Following the investigation using synthesized data, the methodologies are compared using measured data that not only contain measurement uncertainties but realistic boundary layer effects. Further, for the

frequencies of primary interest in this study (i.e., $f \leq 2.6$ kHz), only the plane wave mode ($n = 0$, and $m = 0$) is cut on in the hard wall sections of the GFIT. However, as many as twenty-one modes ($n = 0, 1, 2$ and $m = 0, 1, 2, 3, 4, 5, 6$) are cut on in the hard wall sections of the CDTR.

A. Synthesized Data Results

Each impedance eduction technique has been tested using data synthesized from the exact mode solution given by Eq. (1). The impedance spectrum used to obtain the synthesized data is depicted in Fig. 6. This impedance spectrum was previously obtained using zero flow ($M = 0.0$) GFIT data

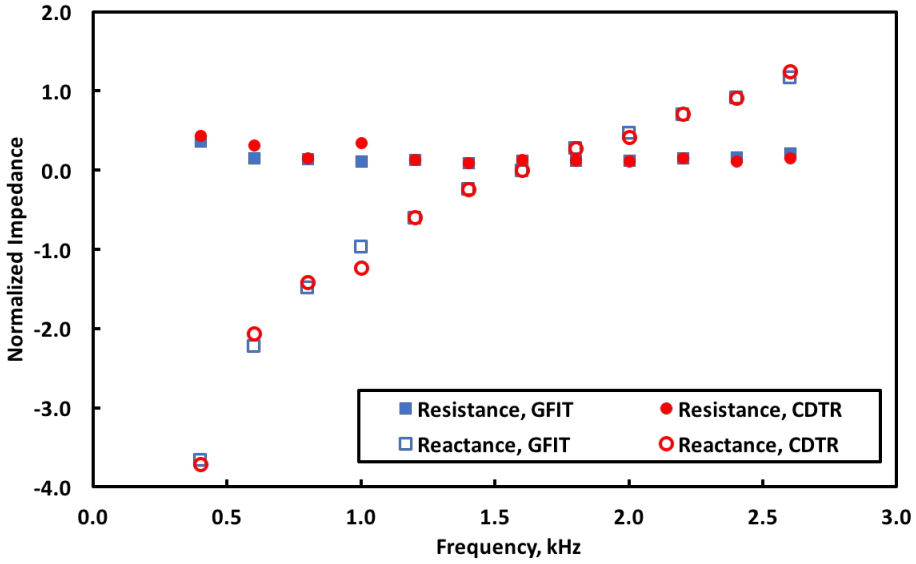

Figure 6. Normalized resistance and reactance spectrum for the conventional liner at Mach 0.0.

with a benchmark method.[1] Throughout this section the normalized impedance of the liner, ζ, is expressed in terms of a two parameter family (its normalized resistance, θ, and its normalized reactance, χ), $\zeta = \theta + i\chi$.

The real and imaginary components of the least attenuated axial wavenumber, K_{0m}, for the impedance spectrum depicted in Fig. 6, are shown in Figs. 7 and 8, respectively, for the GFIT geometry. In these two figures, the least attenuated, axial wave number spectra for two nominal centerline Mach numbers (M =0.0, and M =0.3) are shown. As the GFIT only supports the zeroth order horizontal mode (i.e., $m = 0$) at these source frequencies and Mach numbers, only the components of the least attenuated axial wavenumber for the zeroth order horizontal mode are plotted. Recall that, due to the different orientations of the GFIT and the CDTR, a horizontal mode in the GFIT corresponds to a vertical mode in the CDTR.

Figure 9 shows the reduction in dB (i.e., the attenuation) produced by the liner for the least attenuated mode in the GFIT. The prediction assumes that the liner extends over a meter of duct (L=1.0 m). Note that at Mach 0.0 and Mach 0.3 this liner provides very little attenuation for

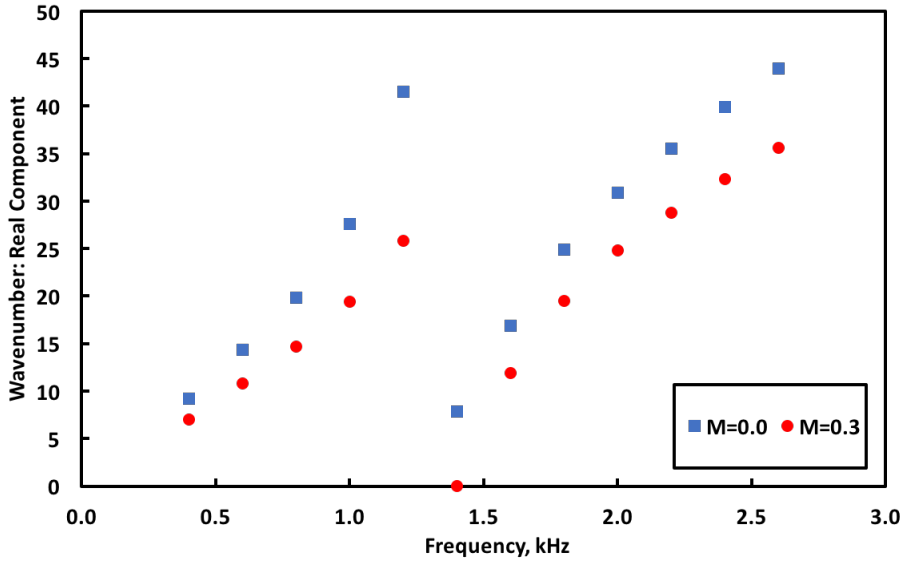

Figure 7. Real component of the axial wavenumber spectra for the conventional liner.

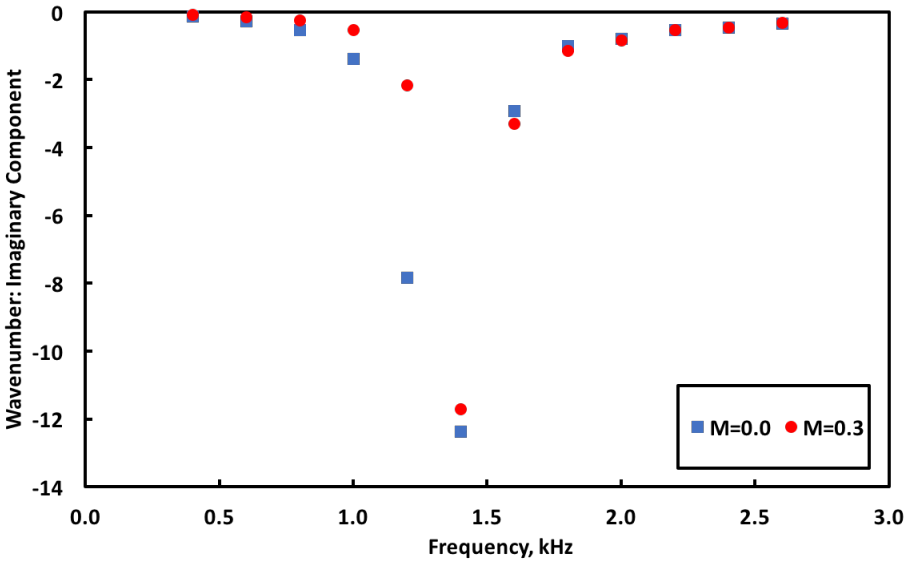

Figure 8. Imaginary component of the axial wavenumber spectra for the conventional liner.

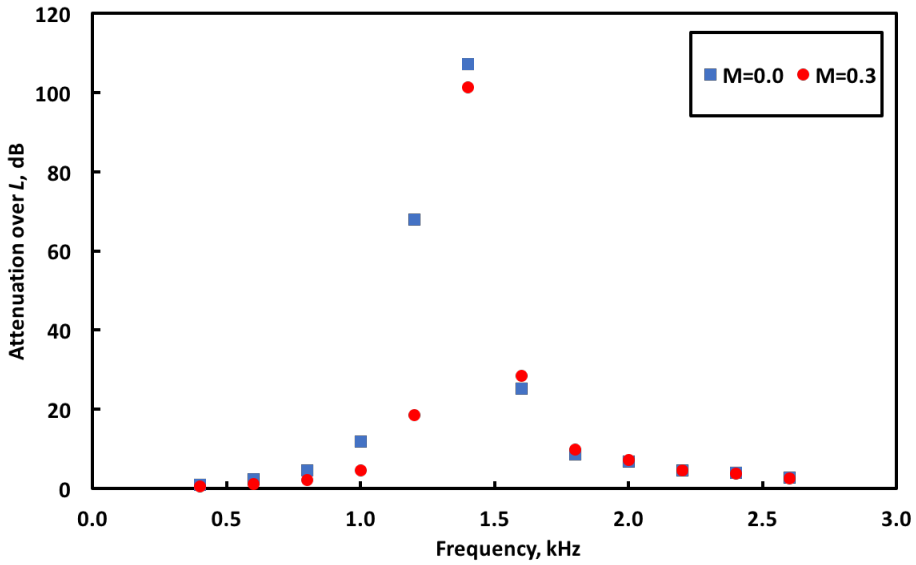

Figure 9. Liner attenuation produced by the conventional liner.

the least attenuated mode at the low frequency end ($f \leq 0.8$ kHz) of the spectra and at the high frequency end ($f \geq 2.4$ kHz) of the spectra. There are large liner attenuations at the frequency of peak attenuation ($f = 1.4$ kHz) at Mach 0.0 and Mach 0.3, respectively.

Figures 10 and 11 compare the educed normalized resistance and reactance spectra, respectively, to that in Fig. 6. Results are given for both the direct method (the KT algorithm) and the

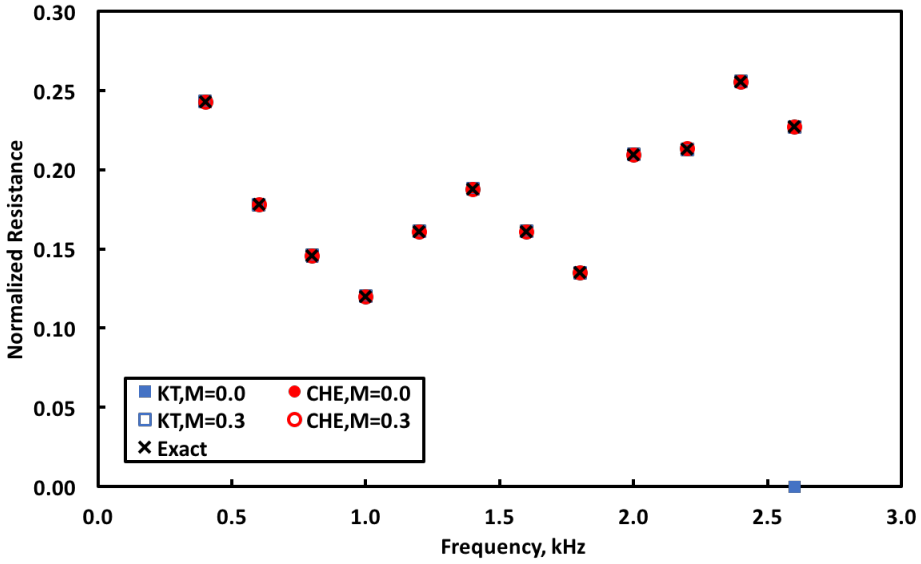

Figure 10. Comparison of the exact normalized resistance with that educed by the KT and CHE methods.

indirect method (the CHE method). Synthesized data for performing the eduction was obtained from the least-attenuated, right-moving mode in Eq. (1). The KT algorithm uses 12 evenly spaced points to sample the acoustic field (for both synthesized and measured data) and the zeroes of an

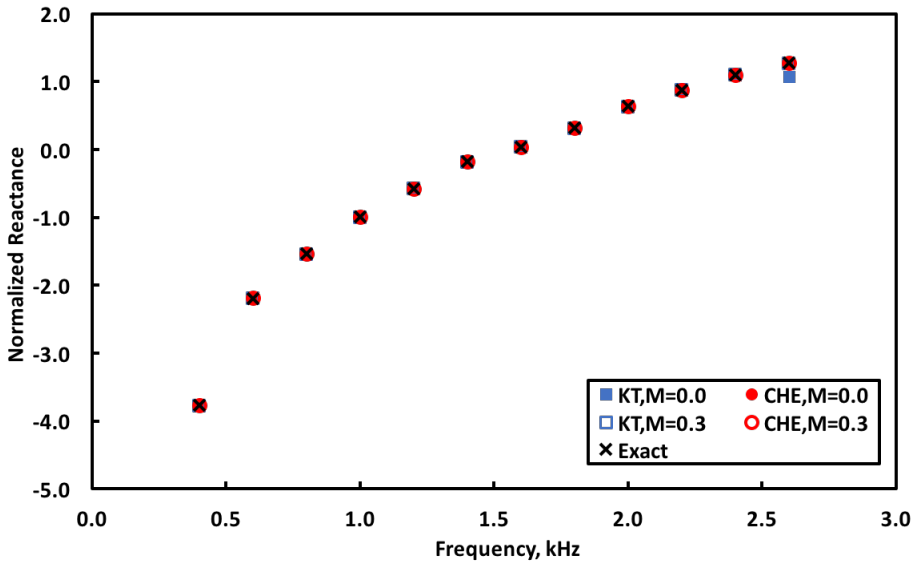

Figure 11. Comparison of the exact normalized reactance with that educed by the KT and CHE methods.

eighth-degree polynomial are used to obtain the axial propagation constant. The finite-element method implemented in the CHE used eighty-one (81) evenly spaced points in the axial direction and twenty-five (25) evenly spaced points between the rigid wall and the liner. As observed in Figs. 10 and 11, both eduction methods overlap with the exact impedance (normalized resistance and reactance) spectrum at each Mach number with one exception. Note that the KT algorithm has educed the incorrect normalized resistance for Mach 0.0 at 2.6 kHz (see Fig. 10). The reason for the failure of the KT algorithm at this condition (i.e., $M = 0.0$ and f=2.6 kHz) is unclear. However, it is believed to be due to the small amount of attenuation produced by the liner at this frequency.

The real and imaginary parts of the least-attenuated axial wavenumber, K_{0m}, for the CDTR geometry are given in Figs. 12 and 13, respectively, for Mach 0.0 and Mach 0.3, and for the first three vertical modes $m = 0, 1, 2$. These axial wavenumbers are obtained using the impedance spectrum given in Fig. 6. Further, they are used to obtain synthesized data for impedance eduction in the CDTR. To validate the two impedance eduction techniques in the CDTR, one needs to show that they educe the same impedance spectrum as that obtained in Fig. 6 for each vertical mode ($m = 0, 1, 2$) and Mach number ($M = 0.0, 0.3$). Recall that for the test frequencies of interest in the CDTR, higher-order vertical modes are cut on and they will need to be taken into account. Thus, the first step in the validation process in the CDTR is to demonstrate that the selected set of 158 microphones is sufficient to perform accurate impedance eductions.

To determine if each impedance eduction method is performing satisfactorily using the selected microphone arrays, we use the axial propagation constants shown in Figs. 12 and 13. Seven hundred and seventy eight (778) equally spaced points are used in the axial direction and sixty-one (61) equally spaced points are used between the rigid left sidewall and the liner in the CHE method. The normalized resistance and reactance spectra educed from the KT and CHE methods were ob-

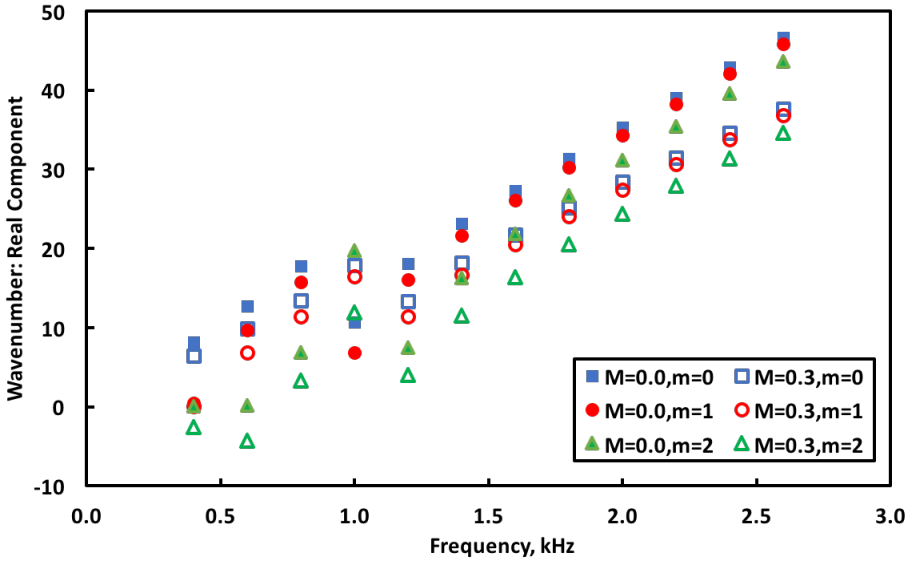

Figure 12. Real component of the least attenuated axial wavenumber for the CDTR.

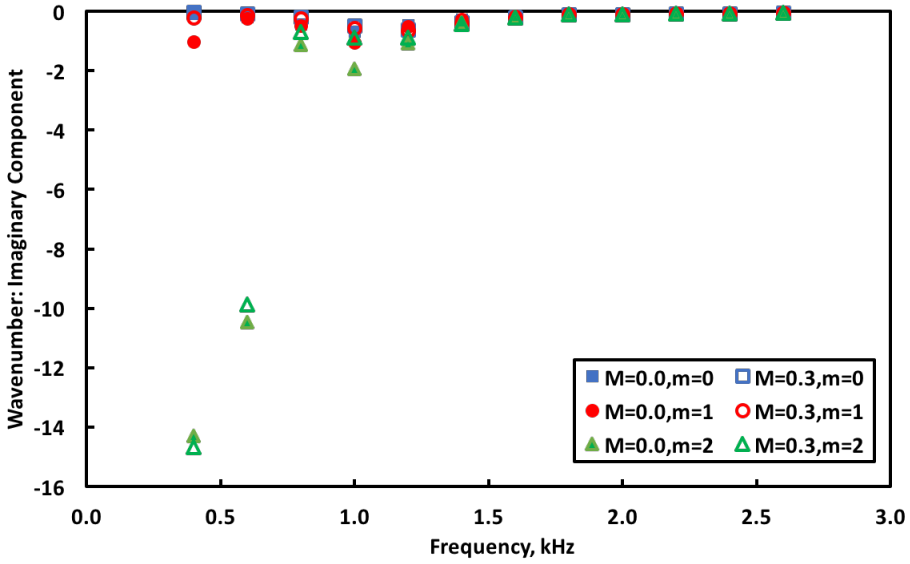

Figure 13. Imaginary component of the least attenuated axial wavenumber for the CDTR.

served to be identical (to within three decimal digits of precision) to that shown in Fig. 6 for each of the three vertical modes orders ($m = 0, 1, 2$) and for each of the two Mach numbers ($M = 0.0$ and $M = 0.3$). These results are not shown for the sake of brevity. Thus, no advantage in accuracy of one impedance eduction method over the other could be detected when data synthesized from the exact mode solution is used. The CHE method is more expensive computationally than the KT algorithm method because the CHE method inverts a matrix and employs an iterative scheme to educe the impedance. However, the CHE method can still be run on a desktop computer within a few minutes of wall clock time. The near perfect agreement of the KT and CHE methods with the impedance spectrum in Fig. 6 is evidence that the chosen microphone locations in the CDTR are sufficient to accurately construct the objective function and educe the impedance by using either impedance eduction methodology.

Unfortunately, the single mode sound fields represented by the axial wavenumbers in Figs. 12 and 13 are not achievable in large facilities such as the CDTR. Reflection of sound from impedance discontinuities along with the cut on of several vertical modes precludes such a simplistic sound field containing only a right-running acoustic mode. There is also measurement error and mean flow gradients that could impact the educed impedance. Mode synthesis is therefore needed to determine the horizontal and vertical mode content in the CDTR. Further, mode synthesis is also needed to determine if a dominant vertical mode is present in the acoustic field. Recall that both the KT algorithm and the CHE method require that a dominant vertical mode be present in the sound field before impedance eduction can be applied using these methodologies. Mode synthesis has been performed on the sound field measured upstream and downstream in the CDTR with the test liner installed. In the hard wall section upstream and downstream of the liner, the solution is expanded as a series of hard wall duct modes:

$$p(x,y,z) = \sum_{n=0}^{nmax} \sum_{m=0}^{mmax} A_{nm}^{\pm} \cos(\frac{n\pi x}{W}) \cos(\frac{m\pi y}{H}) e^{-iK_{nm}^{\pm} z} \tag{12}$$

Evaluating Eq. (12) at each microphone location (x_I, y_I, z_I) gives:

$$p(x_I,y_I,z_I) = \sum_{n=0}^{nmax} \sum_{m=0}^{mmax} A_{nm}^{\pm} \cos(\frac{n\pi x_I}{W}) \cos(\frac{m\pi y_I}{H}) e^{-iK_{nm}^{\pm} z_I}, \quad (I = 1,2,\ldots 63) \tag{13}$$

Equation (13) constitutes a system of 63 equations in $2(nmax+1)(mmax+1)$ unknown mode coefficients for both the upstream and downstream microphone arrays. This system is expressed as a matrix equation of the form

$$[C]\{A^{\pm}\} = \{P\} \tag{14}$$

where $\{A^{\pm}\}$ is a vector containing the $2(nmax+1)(mmax+1)$ mode coefficients, $A_{nm}^{\pm}$. The matrix $[C]$ is a rectangular matrix with N rows and $2(nmax+1)(mmax+1)$ columns. The coefficients

of $[C]$ contain the triple products of hard wall duct modes in the two coordinate directions and an exponential term (i.e., $\cos(\frac{n\pi x}{W})\cos(\frac{m\pi y}{H})e^{-iK^{\pm}_{nm}z}$). This triple product is evaluated at the N microphone locations, $x = x_I, y = y_I$, and $z = z_I$ ($I = 1, 2, \ldots N$). The solution to Eq. (14) is obtained using singular value decomposition

$$\{A^{\pm}\} = [C]^{-1}\{P\} \tag{15}$$

where $[C]^{-1}$ is the pseudo-inverse of the rectangular matrix $[C]$.

By performing the mode synthesis presented in the foregoing paragraph, one can determine if a vertical mode is dominant in the CDTR. To this end, the CDTR control system was used to drive several vertical modes down the CDTR with the objectives of getting a minimal separation (difference in SPL between the mode coefficients of the driven mode and that of all other vertical mode orders) of at least 10 dB. This minimal separation was observed to be achieved when the three lowest order vertical modes (i.e., the (0,0), (0,1), and the (0,2)) were targeted individually by the CDTR control system as the dominant source mode. This minimal separation was achieved in the hard wall sections of duct both upstream and downstream of the liner test section. At most of the test frequencies between 0.4 and 2.6 kHz, the separation was upward of 20 dB in the upstream hard wall section. Recall that an underlying assumption of the KT algorithm and the CHE method is that the targeted m order must be dominant from the source plane to the exit or termination plane of the duct. Thus, if the mode separation is insufficient in either the upstream or downstream hard wall section of the duct, the primary assumption of the higher-order mode impedance eduction theories are not satisfied.

B. Measured Data Results

Impedance spectra are also educed using measured data acquired in the GFIT and CDTR with nearly identical samples. The tests were conducted at an incident SPL level of 130 dB. These tests were conducted with a tonal source (one frequency at a time), at frequencies of 0.4 to 2.6 kHz in 0.2 kHz increments and at two nominal centerline Mach numbers ($M = 0.0$ and $M = 0.3$).

Figures 14 and 15 show educed impedance spectra (normalized resistance and normalized reactance) obtained from measured GFIT data at Mach 0.0 and Mach 0.3, respectively. Results are given for both the KT and CHE impedance eduction methods. Recall that only the plane wave horizontal mode ($m = 0$) is assumed cut on at these frequencies and Mach numbers in the GFIT. Both the KT and CHE methods educed normalized resistance and reactance exhibit the expected trends. That is, the liner has a low normalized resistance of approximately 0.1 at Mach 0.0 and it increases to approximately 0.9 at Mach 0.3. The normalized reactance follows a $-cot(kd)$ behavior. Overall, the educed normalized resistance and reactance from the KT and CHE methods are observed to be extremely close except at the extreme high (i.e., 2.6 kHz) and the extreme low (0.4

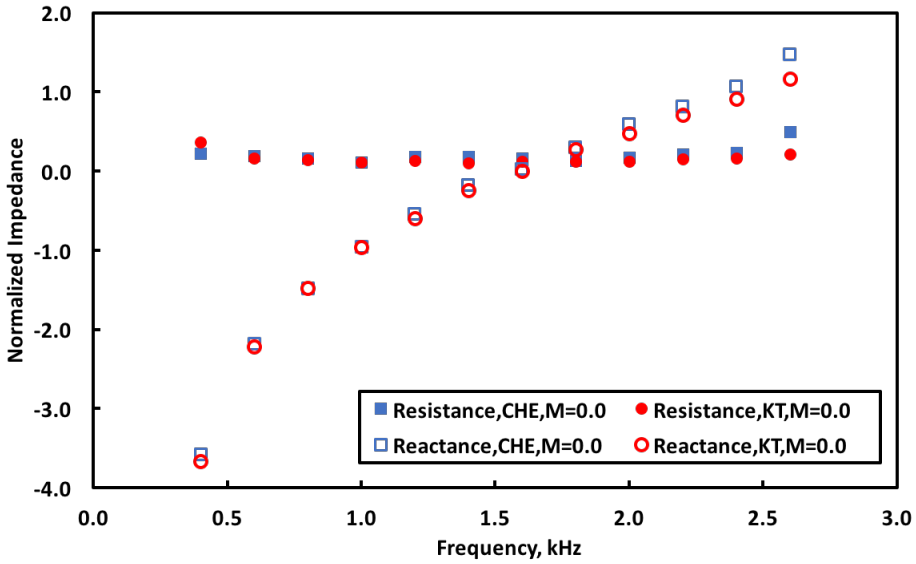

Figure 14. Comparison of the normalized resistance and reactance spectrum educed by the KT and CHE methods in the GFIT at Mach 0.0.

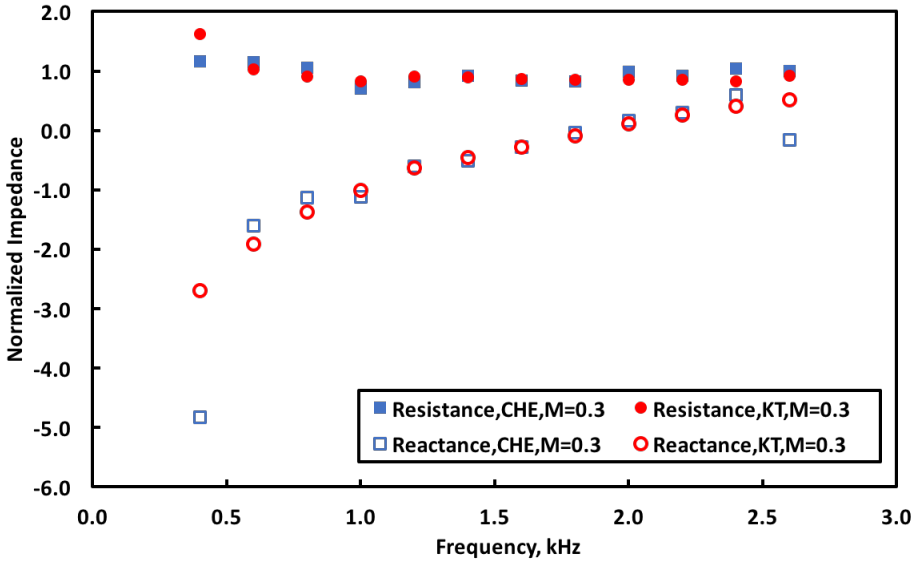

Figure 15. Comparison of the normalized resistance and reactance educed by the KT and CHE methods in the GFIT at Mach 0.3.

kHz) frequency ends of the spectrum at Mach 0.3. These discrepancies were expected. At the high frequency end of the spectra at Mach 0.3 a higher-order mode is nearly cut on so the assumption of a plane wave source in the GFIT is violated. At the low frequency end of the spectrum at Mach 0.3 the attenuation may be too low for adequate impedance eduction. Further, even at this Mach number there may be some effect of the mean boundary layer that has been neglected. Generally speaking, such good overall agreement in educed impedance between the KT and CHE methods as illustrated in Figs. 14 and 15 is extremely encouraging and gives further credence to the impedance eduction techniques.

During the course of this investigation, the KT algorithm was not as reliable when used with measured data as with synthesized data in computing the axial wavenumber. With synthesized data and the eighth-degree polynomial there were eight poles identified by the KT algorithm. Seven of the eight poles were spurious (i.e., did not produce the correct impedance). However, these seven spurious poles could all be identified a priori because their pole magnitude was always less than unity, while the pole corresponding to the liner impedance was easily identified because it had a magnitude greater than unity. However, with the measurement uncertainties and mode scattering present in measured data, the KT algorithm was observed to produce some poles that were spurious with pole magnitudes greater than unity. When using the KT algorithm method, considerable discretion is often required to identify the correct poles associated with the liner impedance in the presence of measured data.

Impedance eductions have also been performed on a sample placed in the CDTR by using the measured CDTR data. Because the KT algorithm is extremely simple and less expensive, results are only presented for the KT algorithm as the CHE method was not run on this data. Three vertical modes ($m = 0, 1, 2$) were isolated by the control system and driven down the CDTR. Figure 16 shows the comparison of the normalized resistance and reactance educed in the GFIT with those educed in the CDTR for the plane wave source in the absence of flow (i.e., $M = 0.0$). Although the acoustic pressure data in the large duct (CDTR) and small duct (GFIT) were different, nearly the same resistance and reactance have been educed. Figure 17 shows similar comparisons but at Mach 0.3 for the plane wave source. Again, good comparison in educed resistance and reactance between the GFIT and CDTR is observed at this Mach number, except at the extreme low frequency end (i.e., 0.4 kHz) and the extreme high frequency end (i.e., 2.6 kHz). The reasons for these discrepancies has been discussed in previous paragraphs.

One surprise not anticipated when higher-order modes were driven in the CDTR was the low amount of attenuation produced by the liner. In the larger duct (i.e., the CDTR) there was very little attenuation of the $m = 1$ and $m = 2$ vertical modes when compared to that of the plane wave mode. Thus, the higher-order modes were not well attenuated except at frequencies of 1.0 kHz, 1.2 kHz, and 1.4 kHz. For source frequencies above 1.4 kHz the liner attenuation is of the order of 1 dB or less. As indicated in other papers,[3,6] the lack of liner attenuation results in poor accuracy

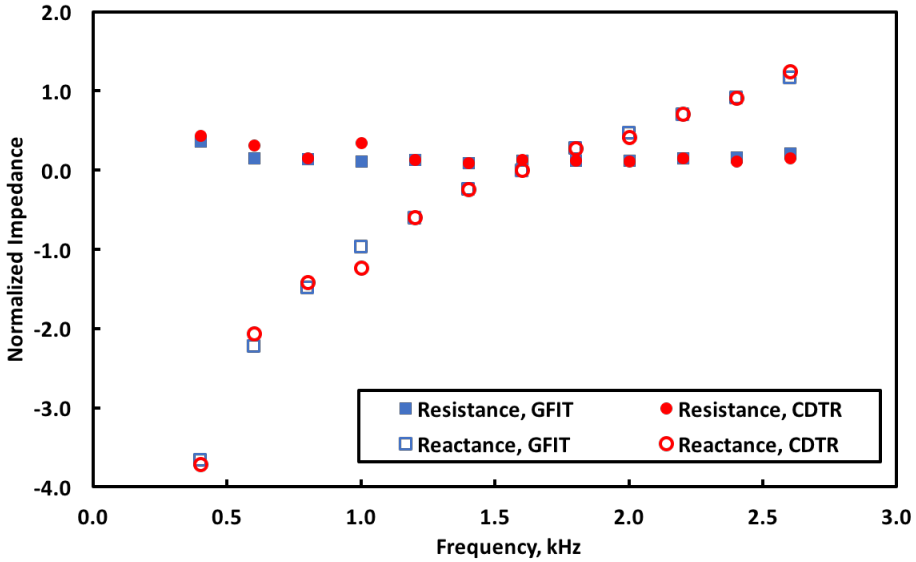

Figure 16. Comparison of the normalized resistance and reactance spectrum educed by the KT algorithm in the GFIT and CDTR at Mach 0.0 using measured data.

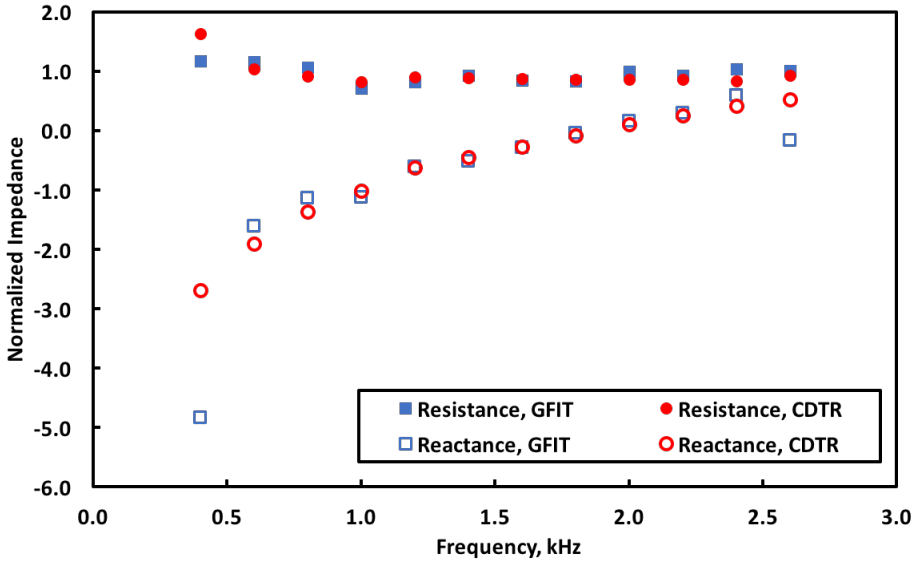

Figure 17. Comparison of the normalized resistance and reactance spectrum educed by the KT algorithm in the GFIT and CDTR at Mach 0.3 using measured data.

in the educed impedance.

Table 1. Comparison of the KT algorithm educed normalized resistance and reactance for the first two vertical modes in the CDTR

f in kHz	Resistance $(m=0)$	Resistance $(m=1)$	Reactance $(m=0)$	Reactance $(m=1)$
0.6	0.16	0.32	-2.06	-2.27
0.8	0.14	0.34	-1.42	-1.6
1.0	0.12	0.39	-1.23	-1.19
1.2	0.13	0.15	-0.60	-0.47
1.4	0.10	0.05	-0.24	-0.40

Table 1 compares the educed normalized resistance and reactance in the CDTR for the first two vertical modes ($m = 0$ and $m = 1$) at the frequencies of highest attenuation (in the absence of flow). The comparison of educed resistance and reactance for the lowest-order vertical mode ($m = 0$) and first-order vertical mode ($m = 1$) is favorable at these frequencies where a reasonable amount of attenuation (3 dB or more) is obtained by the liner. Trends similar to those in Table 1, were observed at Mach 0.3, although the quality of the comparisons degraded slightly because the larger Mach number reduced the attenuation of the liner. Similar studies to those in Table 1 are being carried out using the CHE method of impedance eduction, but the results of this study are beyond the scope of the current paper.

VII. Conclusions

Based on the results of this study, the following conclusions are drawn:

1. The KT algorithm and the CHE method of impedance eduction have been validated by placing a liner sample in a duct with a large cross-sectional area (the CDTR) and a second liner sample (with the same liner parameters) in a duct with a much smaller cross-sectional area (the GFIT). The same impedance spectra are educed by each method under identical test conditions. This was confirmed first using data synthesized from an exact mode solution and second with measured data for a plane wave source in the GFIT.

2. The higher-order modes see the same locally-reacting impedance as the plane wave mode at the liner surface in a grazing flow environment (when there is sufficient attenuation by the liner). This could only be demonstrated in the large duct where a higher-order vertical mode was not only cut on but could be well separated from other vertical modes by the control system. This has been demonstrated for each of the two impedance eduction techniques by

using data synthesized from an exact mode solution and also with measured data.

The success of the CHE method in this paper motivates its use to educe impedance in samples with variable impedance liners. A similar statement can be made for the KT algorithm although it is limited to uniform impedance samples.

Acknowledgment

The NASA Fixed Wing Project of the Fundamental Aeronautics Program funded this research.

References

[1]Watson, W. R., Jones, M. G., and Parrott, T. L., "Validation of an Impedance Eduction Method in Flow," *AIAA Journal*, Vol. 37, No. 7, July 1999, pp. 818−824.

[2]Jones, M. G., Watson, W. R., Tracy, M. B., Parrott, T. L., "Comparison of Two Waveguide Methods for Educing Liner Impedance in Grazing Flow," *AIAA Journal*, Vol. 42, No. 2, Feb. 2004, pp. 232−240.

[3]Jones, M., Watson, W., and Parrott, T., "Benchmark Data for Evaluation of Aeroacoustic Propagation Codes with Grazing Flow." AIAA Paper 2005−2853, May 2005.

[4]Watson, W. R., Jones, M. G., and Parrott, T. L., "Comparison of a Convected Helmholtz and Euler Model for Impedance Eduction in Flow," AIAA paper 2006-2643, May 2006.

[5]Jones, M. G., Watson, W. R., and Nark, D. M., "Effects of Flow Profile on Educed Acoustic Liner Impedance," AIAA Paper 2010-3763, June 2010.

[6]Watson, W. R., and Jones, M. G., "A Comparative Study of Four Impedance Eduction Methodologies Using Several Test Liners." AIAA Paper 2013-2274, June 2013.

[7]Gerhold, C., Cabell, R., and Brown, M., "Development of an Experimental Rig for Investigation of Higher-Order Modes in Ducts," AIAA Paper 2006-2637, May 2006.

[8]Gerhold, C. H., Brown, M. C., Jones, M. G., and Howerton, B. H., "Report on Recent Upgrades to the Curved Duct Test Rig at NASA Langley Research Center," AIAA Paper 2011-2896, June 2011.

[9]Watson, W. R., Jones, M. G., and June, J. C., "Single Mode Theory for Impedance Eduction in Large-Scale Ducts with Grazing Flow," AIAA Paper 2014−3351, June 2014.

[10]Kumaresan, R. and Tufts D., "Estimating the parameters of exponentially damped sinusoids and pole-zero modeling in noise," *IEEE Trans. Acoust., Speech, Signal Process*, Vol. 30, Dec. 1982, pp. 833 − 840.

[11]Watson, W. R., Carpenter, M. H., and Jones, M. G., " Performance of Kumaresan and Tufts Algorithm in Liner Impedance Eduction with Flow," *AIAA Journal*, Vol. 53, No. 4, Feb. 2015, pp. 1091−1102.

[12]Myers, M. K.,"On The Acoustic Boundary Condition In The Presence Of Flow," *Journal Of Sound And Vibrations*, Vol. 71 No. 3 , Aug. 1980, pp. 429−434,.

[13]Stewart, G. W., III, "A Modification of Davidon's Minimization Method to Accept Difference Approximations of Derivatives," *Journal of ACM*, Vol. 14, No. 1, 1967, pp. 72−83.

[14]Watson, W. R. and Jones, M. G. "Impedance Eduction in 3D Sounds Fields with Peripherally Varying Liners and Flow," AIAA Paper 2015-2228, June 2015.